

Constraint Dependence of Active Depletion Forces on Passive Particles

Peng Liu,^{1,2,*} Simin Ye,^{1,2,*} Fangfu Ye,^{1,2,3,4,†} Ke Chen,^{1,2,4,‡} and Mingcheng Yang^{1,2,§}

¹Beijing National Laboratory for Condensed Matter Physics and Laboratory of Soft Matter Physics, Institute of Physics, Chinese Academy of Sciences, Beijing 100190, China

²School of Physical Sciences, University of Chinese Academy of Sciences, Beijing 100049, China

³Wenzhou Institute, University of Chinese Academy of Sciences, Wenzhou, Zhejiang 325001, China

⁴Songshan Lake Materials Laboratory, Dongguan, Guangdong 523808, China



(Received 6 September 2019; revised manuscript received 22 February 2020; accepted 25 March 2020; published 13 April 2020)

Using simulations and experiments, we demonstrate that the effective interaction between passive particles in an active bath substantially depends on an external constraint suffered by the passive particles. Particularly, the effective interaction between two free passive particles, which is directly measured in simulation, is qualitatively different from the one between two fixed particles. Moreover, we find that the friction experienced by the passive particles—a kinematic constraint—similarly influences the effective interaction. These remarkable features are in significant contrast to the equilibrium cases, and mainly arise from the accumulation of the active particles near the concave gap formed by the passive spheres. This constraint dependence not only deepens our understanding of the “active depletion force,” but also provides an additional tool to tune the effective interactions in an active bath.

DOI: [10.1103/PhysRevLett.124.158001](https://doi.org/10.1103/PhysRevLett.124.158001)

Introduction.—Active matters consisting of self-propelled units are an important class of nonequilibrium systems, ranging from cell cytoskeleton [1,2] to biological and artificial microswimmers [3–12] to shaken grains [13–16]. Active matter systems often exhibit exotic behaviors not found in passive systems, including complex collective motions [17–24], motility-induced phase separation [25–27], or wall-dependent pressure [28,29]. Apart from the emergence of intriguing nonequilibrium phenomena, an active bath can significantly affect immersed passive objects compared to an equilibrium bath. For instance, active environment can enhance diffusion and effective temperature of tracer particles [30–32], power a directed motion of asymmetric objects [33–36], dramatically deform flexible macromolecules [37–42], and induce unexpected self-assemblies and phase separations of passive colloids [43–47]. To exploit these nonequilibrium behaviors of immersed passive particles, it is fundamentally important to understand interparticle effective interaction mediated by the active bath, i.e., active depletion force.

The active depletion force is a conceptual generalization of the equilibrium depletion force [48–53] that is an effective interaction between large particles suspended in an overwhelming number of smaller particles or depletants, and arises from the gain of the system entropy dominated by the depletants by compressing the phase space of the large particles. In active systems, however, this entropy scenario is no longer applicable.

Recently, the active depletion interactions are either characterized from pair correlation function, $g(r)$ of unconstrained passive particles [44,54–56] or determined by

measuring the forces, $\mathbf{F}_{\text{eff}}(r)$, exerted on two fixed objects by the active bath [29,55,57–63]. In equilibrium systems, the effective force and the pair correlation function are directly related by $\mathbf{F}_{\text{eff}}(r) = k_B T \nabla \ln[g(r)] - \mathbf{F}_r(r)$, with $\mathbf{F}_r(r)$ the steric interaction between passive particles. This relation, however, is likely to fail in an active bath, which is far from equilibrium. More importantly, it is not clear at all whether either method obtains the true effective forces experienced by free passive particles in an active bath, the driving force for self-assemblies or phase behaviors in the nonequilibrium systems.

In this Letter, we directly measure the active depletion forces between two passive particles in steady states, using computer simulations and laser tweezer experiments. We find that the effective force on the free passive particle clearly deviates from that inferred from $g(r)$. By constraining the passive particles under external traps, we demonstrate that the active depletion force sensitively depends on the degree of the constraint, thus the $\mathbf{F}_{\text{eff}}(r)$ on a free object is qualitatively different from the fixed case. In addition, the active depletion forces for free passive objects vary with their frictional coefficients that impose kinematic constraints. Microscopically, the constraint-dependent effective forces come from the fact that the distribution of active depletant near passive objects depends sensitively on the constraints of the objects. Our results thus indicate that the active depletion is much more complex than expected and cannot be treated in the same fashion as in equilibrium systems.

Simulation.—We consider a 2D system consisting of 1000 small self-propelled particles of diameter σ_s and two

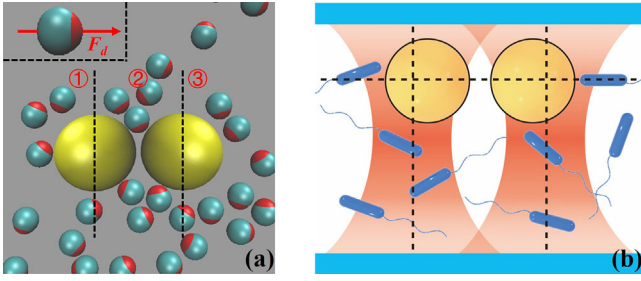


FIG. 1. (a) Sketch of simulation system, consisting of small active particles self-propelling toward the red side and two large (yellow) passive particles. Two vertical dashed lines mark three different regions around the passive particles, in which the active particles contribute differently to depletion force. (b) Schematic experimental system with PS particles (yellow) trapped optically in bacteria solution. The observing plane and trap centers are marked by dashed lines.

large passive particles of diameter $\sigma_l = 3\sigma_s$, as sketched in Fig. 1(a). All particles interact with each other through a repulsive Lennard-Jones type of potential, $U(r) = 4\epsilon[(\sigma/r)^{24} - (\sigma/r)^{12}] + \epsilon$ for $r < 2^{1/12}\sigma$. Here, the interaction diameter between the passive and active particles is taken as $\sigma = (\sigma_s + \sigma_l)/2$. The translational dynamics of the active particles is described by overdamped Langevin equation, $\gamma_s \mathbf{v} = \mathbf{F}_d + \mathbf{F}_r + \boldsymbol{\eta}$, where γ_s is the translational friction coefficients, \mathbf{F}_d the self-propelling force, \mathbf{F}_r the steric interaction between particles, and $\boldsymbol{\eta}$ the Gaussian-distributed stochastic force of zero mean and variance $\langle \boldsymbol{\eta}(t)\boldsymbol{\eta}(t') \rangle = 2k_B T \gamma_s \delta(t - t')$ with $k_B T = \epsilon$. The orientation of the active particles evolves according to rotational diffusion, with the rotational frictional coefficient $\gamma_r = \frac{1}{3}\sigma_s^2 \gamma_s$ unless otherwise stated. The dynamics of the isotropic passive particles also obeys an overdamped Langevin equation, with the frictional coefficient γ_l and $\mathbf{F}_d = 0$. When considering the passive particles in confinement, an external trapping potential, $U_{\text{ex}}(\mathbf{r}) = \frac{1}{2}k_{\text{el}}(\mathbf{r} - \mathbf{r}_0)^2$, is applied with \mathbf{r}_0 the trap center.

Measurement of the depletion force.—In simulations, the $\mathbf{F}_{\text{eff}}(r)$ is directly measured by accumulating the average force on the free passive particles exerted by the active particles in a small range of separation around r in the steady state. Generally, this accumulated mean force includes the total depletion force, and partial frictional and stochastic forces experienced by the passive particle (thermal bath also contributes to frictional and stochastic forces), which prevents the extraction of $\mathbf{F}_{\text{eff}}(r)$. However, when particle distribution reaches the steady state, the passive particle flux and hence the friction vanish. The averaged stochastic force is also zero at steady state. In the nonequilibrium steady state, the nonuniform pressure and swimmer density, arising from the anisotropic interactions between the active swimmers and the passive particle pair, may spontaneously generate a local current of swimmers [40]. This current, however, does not contribute to the

friction on the passive particles, as it is self-generated instead of externally imposed and is an accompanying effect of the active depletion interaction. Thus, the average force measured at steady states can be exclusively attributed to the active depletion force. The method is valid in both equilibrium and nonequilibrium systems, and has been demonstrated in simulations by computing equilibrium depletion forces (see the Supplemental Material [64]) and thermophoretic force in nonisothermal solutions [71]. This procedure can also be used to measure $\mathbf{F}_{\text{eff}}(r)$ on passive particles in elastic traps when the passive particles fluctuate close to their equilibrium positions. Fixing passive objects, corresponding to infinitely strong traps, also eliminates the friction but it drastically changes the particle dynamics, which may affect the active depletion interactions.

Experiment.—A dilute dispersion of polystyrene (PS) beads of diameter $\sigma_l = 3 \mu\text{m}$ is mixed with a solution of E.coli bacteria ($\sigma_s = 0.6 \mu\text{m}$ in diameter, $4\sigma_s$ in length, with a swimming speed $\sim 20 \mu\text{m/s}$), and is then loaded into a glass cell with a thickness of $30 \mu\text{m}$. Two PS particles are trapped near the upper cover slide by two identical optical tweezers (Aresis Tweez 250si) at the same height, as sketched in Fig. 1(b). The laser intensity is low such that the number density and motility of the bacteria are hardly affected by the irradiation. The PS particles are confined to fluctuate around a separation r without direct contact. In the steady state, the active depletion forces on the particles from the surrounding bacteria shift the particle equilibrium positions slightly away from the trap centers. Each particle may also experience a small attraction from the optical trap of the other particle. After calibration, the depletion forces on the PS particles can be extracted from the particle positions (see the Supplemental Material [64]). By tuning the separation of two optical traps and the laser intensity, we obtain the $\mathbf{F}_{\text{eff}}(r)$ as a function of r and the trap stiffness, respectively.

Results and discussion.—We first perform simulations to study the effect of constraint on $\mathbf{F}_{\text{eff}}(r)$. The dimensionless stiffness coefficient, $k = k_{\text{el}}\sigma_s^2/k_B T$, of the trap potential is tuned from 0 (free) to infinity (frozen). In the simulations, we choose the packing fraction of active particles $\rho = 0.2$ to avoid the formation of large clusters, and the reduced self-propelling force $\mathbf{F}_d\sigma_s/k_B T = 20$. Figure 2(a) plots the measured \mathbf{F}_{eff} as a function of particle separation r and stiffness coefficient k . It is clear that the $\mathbf{F}_{\text{eff}}(r)$ on the passive particles strongly depends on the stiffness coefficient, in stark contrast to equilibrium cases where depletion forces are independent of constraints. For the free passive particles, $\mathbf{F}_{\text{eff}}(r)$ has a strong attraction at $r \simeq \sigma_l$ and a small peak of repulsion at $r \simeq \sigma_l + 0.8\sigma_s$; while the frozen case exhibits reverse properties, a weak attraction and a strong repulsive peak. This observation is consistent with previous work, where free passive objects in an active bath aggregate together [44,54,56] while fixed ones exhibit

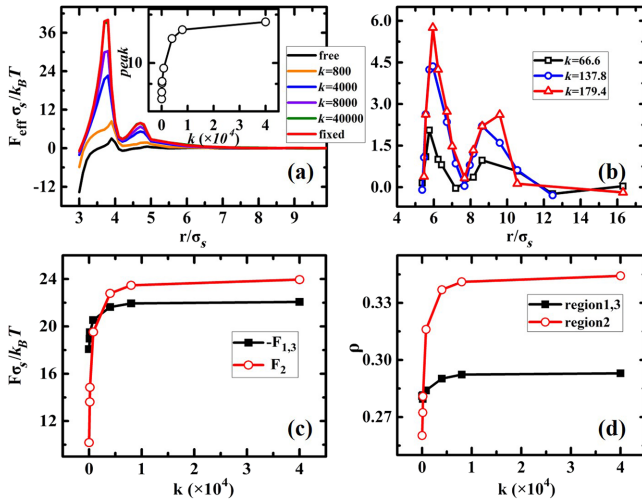


FIG. 2. Reduced effective force as a function of the distance between passive particles for various trap stiffness in simulation (a) and experiment (b), with negative forces being attraction. The inset in (a) shows the maximum of F_{eff} versus trap stiffness. (c) Magnitudes of $F_{1,3}$ and F_2 , and (d) packing fractions of swimmers in different regions versus trap stiffness.

a strong repulsion [29,55,59,60]. The whole profile of $F_{\text{eff}}(r)$ rises (becomes more repulsive) with k , and saturates at the largest k [inset of Fig. 2(a)].

The profile of $F_{\text{eff}}(r)$ and its dependence on constraints can be understood by analyzing the distribution of active depletants in different regions near the passive particles. As illustrated in Fig. 1(a), collisions occurring in regions 1 and 3 generate effective attractions between the passive spheres $F_{1,3}(r)$; while swimmers in region 2 tend to push the two passive spheres apart, thus generating repulsions $F_2(r)$. The total depletion force is then the result of competition of the attractive and repulsive forces, $F_{\text{eff}}(r) = F_{1,3}(r) + F_2(r)$. Moreover, due to their persistence of motion, the swimmers are more easily trapped and temporarily accumulated in the concave region 2 than in the convex region 1 or 3 [55,59,72]. At small r ($\approx \sigma_l$), the concave area between two passive particles is small with lower number of swimmers in region 2 than region 1 or 3, and so the $F_{\text{eff}}(r)$ is attractive. The concave area increases with r , while the collision area in regions 1 and 3 remains constant. Thus, the repulsive force from the accumulation of active depletants in region 2 eventually dominates the $F_{\text{eff}}(r)$ that reaches a maximum at $r < \sigma_l + \sigma_s$. Further increasing the separation creates a gap that allows one swimmer to easily pass through without being trapped, which sharply reduces the $F_2(r)$. For $r \leq \sigma_l + 2\sigma_s$, the gap between the passive spheres can be temporarily jammed by two swimmers with a certain probability, leading to an increase of $F_2(r)$ manifested in the second and weaker peak in Fig. 2(a). At larger r , a dynamic bridge composed of multiple layers of swimmers cannot be maintained in the gap in dilute suspensions [58]; the environments in the three regions become equivalent, and the $F_{\text{eff}}(r)$ vanishes.

The constraints on the passive particles mainly influence the repulsive force from region 2. Under weak or zero constraints, the swimmers in region 2 can easily push through the gap between the passive objects, such that the collision process is similar to that in regions 1 or 3. Under strong constraints, the passive spheres lack a sufficient displacement within the orientational diffusion time of swimmer, which leads to a strong accumulation of the swimmers in the concave region 2. The accumulated swimmers greatly enhance $F_2(r)$, and hence the total effective force becomes increasingly repulsive with k [Fig. 2(a)]. We verify the above scenario by directly quantifying the repulsive (F_2) and attractive ($F_{1,3}$) forces exerted on the passive particle and the corresponding swimmer packing fractions in region 2 and regions 1,3, as a function of the trap stiffness k , for passive particle separation $r/\sigma_s = 3.1$. As shown in Figs. 2(c) and 2(d), the repulsive force and the packing fraction in region 2 increase more rapidly with k than their counterparts in regions 1,3, driving the overall active depletion force from attractive to repulsive. The transition stiffness coefficient, $k \approx 2000$, where F_{eff} changes the sign ($F_{1,3} + F_2 = 0$), is higher than that inferred from the packing fraction profiles, $k \approx 400$, where ρ in regions 1,3 and region 2 become equal. This apparent discrepancy arises from the different collision intensities on single swimmer level in regions 1,3 and region 2. The swimmers colliding with the passive particles in regions 1,3 are more likely to orientate parallel to the F_{eff} , thus on average, generating a larger force per collision, which requires a higher swimmer concentration in region 2 (larger k) to completely balance the $F_{1,3}$.

Our simulation results are verified by laser tweezer experiments with PS particles and *E. coli* bacteria. In the experiments, the dimensionless self-propelled force is estimated to be $F_d \sigma_s / k_B T = 19.3$ (σ_s the bacterial diameter), close to that in the simulations. The packing fraction of the bacteria near the focal plane is $\rho \approx 0.048$. Considering the 3D experimental system, the evaluated effective 2D packing fraction is comparable to the simulation (see the Supplemental Material [64]). Figure 2(b) plots the measured effective interaction between the PS spheres as a function of particle separation and trap stiffness. The experiments demonstrate that the $F_{\text{eff}}(r)$ increases with the constraint, consistent with the simulations. Similar to the simulations, two repulsive peaks are observed in the experiments for all three stiffness coefficients. The first peak corresponds to the maximum gap ($r \leq \sigma_l + \sigma_s$) between PS particles that forbids a bacteria to pass. The peak values of the active depletion forces are separately 2.1, 4.4, and 5.8 for $k \approx 67$, 138, and 180, comparable to the simulation results for the same set of trap stiffness with peak values at 3.8, 5.1, and 5.4, respectively [inset of Fig. 2(a)]. The second peak corresponds to the maximum concave region ($r \leq \sigma_l + 4\sigma_s$) that does not allow the bacteria to pass through laterally (with its long

axis) but is freely permeable to the bacteria swimming longitudinally, as the bacteria are rod shaped. The agreement between simulation results and experimental observations suggests that hydrodynamic interactions, which is lacking in the simulations, and the swimmer shape (sphere in simulation, and rodlike in experiment) probably play lesser roles for active depletion interaction. To better mimic the motion of bacteria in experiment, we perform simulations with the run-and-tumble dynamics, and obtain qualitatively the same results (see the Supplemental Material [64]).

The strong constraint dependence of active depletion force shows that the $\mathbf{F}_{\text{eff}}(r)$ on free passive particles cannot be obtained from frozen particles. We also examine the feasibility of deriving the $\mathbf{F}_{\text{eff}}(r)$ using $k_B T \nabla \ln[g(r)]$, with $g(r)$ the pair correlation function of the free passive particles in the active bath. The depletion force derived from $g(r)$ is plotted in Fig. 3(a) (pink line with circles) with the thermal bath temperature, significantly different from that obtained from direct measurement (olive line). The derived $\mathbf{F}_{\text{eff}}(r)$, however, exhibits a similar trend to the measured force curve. It thus seems possible to employ an effective temperature to scale the derived forces to the true $\mathbf{F}_{\text{eff}}(r)$. The best-fitted profile yields an effective temperature around $0.6T$ and still shows clear discrepancies from the measured force near the attractive well (see the Supplemental Material [64]). An effective temperature less than T obviously disagrees with the conventional wisdom that a passive particle in an active bath should have a higher effective temperature than in an equilibrium bath [31,32]. Therefore, $g(r)$ cannot be reliably employed to extract the active depletion forces with *a priori* effective temperature higher than T , obtained independently from common routes. The pair correlation function can, however, qualitatively determine the sign of active depletion forces for free passive particles. The experimental $g(r)$ of free PS particles in an active bacterial bath shows a pronounced peak, indicating an attractive $\mathbf{F}_{\text{eff}}(r)$ between the passive PS particles, in agreement with the simulations (see the Supplemental Material [64]).

By exploring wider parameter spaces, we further demonstrate that $\mathbf{F}_{\text{eff}}(r)$ on free and fixed passive particles are essentially different (Fig. 3). Moreover, Figs. 3(a)–3(c) and 3(e) show that the magnitudes of $\mathbf{F}_{\text{eff}}(r)$ for both free and fixed cases increase with the swimmer driving force, packing fraction and rotational timescale (represented as the Peclet number $\text{Pe} = (\mathbf{F}_d \gamma_r / k_B T \sigma_s \gamma_s)$ with constant \mathbf{F}_d), as both $\mathbf{F}_{1,3}(r)$ and $\mathbf{F}_2(r)$ are, respectively, increasing functions of \mathbf{F}_d , ρ and swimmer-particle interacting duration. The increase of $\mathbf{F}_{\text{eff}}(r)$ with depletant concentration is verified by experiments [Fig. 3(d)]. Although the γ_r and \mathbf{F}_d dependences of $\mathbf{F}_{\text{eff}}(r)$ are similar, their effects on $\mathbf{F}_{\text{eff}}(r)$ are not quantitatively equivalent. For instance, the system with $\mathbf{F}_d \sigma_s / k_B T = 60$ in Fig. 3(b) has $\text{Pe} = 20$, but its repulsive peak is three times of its counterpart in Fig. 3(e).

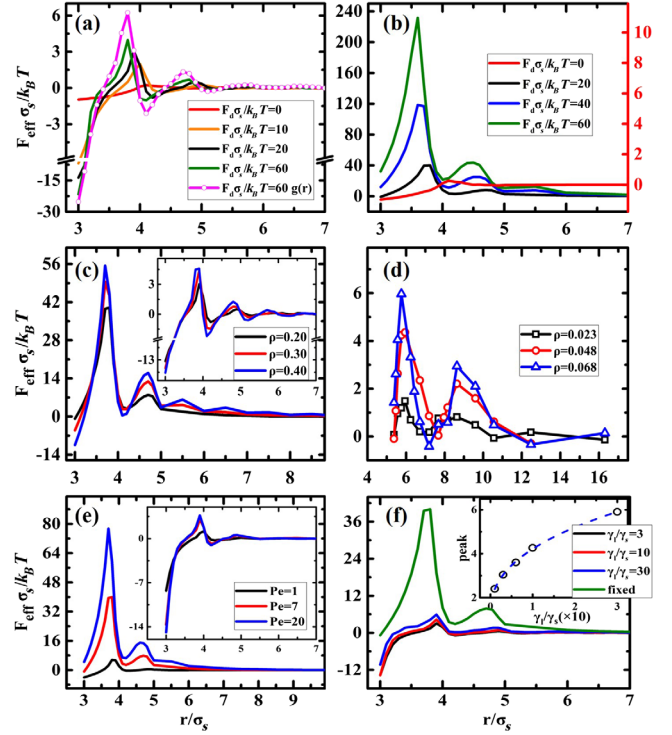


FIG. 3. Reduced effective forces on free (a) and frozen (b) passive particles for different driving forces on swimmers, with $\rho = 0.2$. The pink line with circles in (a) refers to $\mathbf{F}_{\text{eff}}(r)$ calculated from $g(r)$ with the thermal bath temperature T , and the right (red) vertical axis in (b) to the passive system. Panel (c) and its inset, respectively, denote $\mathbf{F}_{\text{eff}}(r)$ on fixed and free passive particles for different swimmer packing fractions in simulations, with $\mathbf{F}_d \sigma_s / k_B T = 20$. (d) Experimental $\mathbf{F}_{\text{eff}}(r)$ for various ρ with $k = 137.8$. Panel (e) and its inset separately denote $\mathbf{F}_{\text{eff}}(r)$ on fixed and free passive particles for different γ_r (Pe), with \mathbf{F}_d fixed. (f) $\mathbf{F}_{\text{eff}}(r)$ on free passive particles of various frictional coefficients γ_l . The olive line is $\mathbf{F}_{\text{eff}}(r)$ on fixed passive particles. The inset shows the repulsive peak of $\mathbf{F}_{\text{eff}}(r)$ versus γ_l , where the dashed line is a fit for extrapolation. In (e) and (f), $\mathbf{F}_d \sigma_s / k_B T = 20$ and $\rho = 0.2$.

This implies that the effects of γ_r and \mathbf{F}_d cannot be reduced to a single Pe. The particle size dependence of $\mathbf{F}_{\text{eff}}(r)$ is provided in the Supplemental Material [64].

We have shown that active depletion force on passive particles strongly depends on their external elastic constraints, which originates from the constraint-modified kinematics of passive spheres and (in turn) nearby swimmers, facilitating the swimmer trapping in the region between the passive particles under strong constraints. Besides the elastic trap, an alternative way to control the kinematics of colloidal body is to change its friction from environment including boundaries and fluids. Similar to a particle under a strong elastic trap, a passive particle with a large friction coefficient cannot move fast enough in response to the impact of swimmers. Higher frictional coefficients of the particles thus effectively correspond to stronger constraints. In simulations, to exclusively study

the effect of the kinematic constraint on $\mathbf{F}_{\text{eff}}(r)$, we change γ_l independently while keeping γ_s constant [Fig. 3(f)]. For comparison, the $\mathbf{F}_{\text{eff}}(r)$ for fixed case is also plotted, which is effectively equivalent to infinite γ_l . With increasing γ_l , all the features of $\mathbf{F}_{\text{eff}}(r)$ under elastic constraints shown in Fig. 2(a) are recovered, implying that the active depletion forces under both elastic and viscous constraints result from similar underlying mechanisms. An interesting question is how large the γ_l needs to be to observe $\mathbf{F}_{\text{eff}}(r)$ on free particles with the same magnitude as that obtained in frozen cases. A rough extrapolation of $\mathbf{F}_{\text{eff}}(r)$ as a function of γ_l yields $\gamma_l = 6 \times 10^4 \gamma_s$, which amounts to the frictional coefficient of a macroscopic sphere of radius 3 cm in water. This further confirms that free mesoscopic colloidal particles in active baths cannot be simply treated as fixed objects.

Conclusion.—By directly measuring the forces in steady states, we show that the active depletion forces on passive colloidal objects in an active bath are greatly influenced by the elastic or kinematic constraints on the objects. The effective interaction changes from a strong attraction to a strong repulsion as the constraint increases. Frozen particles cannot be employed as force probes to estimate the active depletion forces on freely moving passive particles. The pair correlation function, which is directly related to effective interparticle potential in equilibrium systems, also fails to quantitatively extract the active depletion forces. The key features of the simulation results are verified in experiments with PS particles optically trapped in bacteria solutions, wherever comparison is possible. Therefore, the active depletion interactions must be properly taken into account, when designing or analyzing activity-directed assembly, phase transition, and transportation of colloids. Our work can be straightforwardly extended to study effective interactions in other diverse active systems.

We thank K. Zhao and Y. W. Zong at Tianjin University for providing the *E. coli* bacteria. We acknowledge support from National Natural Science Foundation of China (Grants No. 11874397, No. 11874395, No. 11674365, No. 11474327, No. 11475018, and No. 11774394). This work was also supported by the MOST 973 Program (No. 2015CB856800) and the Key Research Program of Frontier Sciences of Chinese Academy of Sciences (Grant No. QYZDB-SSW-SYS003).

*These authors contributed equally to this work.

[†]fye@iphy.ac.cn

[‡]kechen@iphy.ac.cn

[§]mcyang@iphy.ac.cn

- [1] M. C. Marchetti, J. F. Joanny, S. Ramaswamy, T. B. Liverpool, J. Prost, M. Rao, and R. A. Simha, *Rev. Mod. Phys.* **85**, 1143 (2013).
 [2] A. Rigato, A. Miyagi, S. Scheuring, and F. Rico, *Nat. Phys.* **13**, 771 (2017).

- [3] H. C. Berg, *E. Coli in Motion, Volume 7 of Biological and Medical Physics* (Springer, New York, 2004).
 [4] H. Wioland, F. G. Woodhouse, J. Dunkel, J. O. Kessler, and R. E. Goldstein, *Phys. Rev. Lett.* **110**, 268102 (2013).
 [5] H. Li, X.-q. Shi, M. Huang, X. Chen, M. Xiao, C. Liu, H. Chaté, and H. Zhang, *Proc. Natl. Acad. Sci. U.S.A.* **116**, 777 (2019).
 [6] C. Bechinger, R. Di Leonardo, H. Löwen, C. Reichhardt, G. Volpe, and G. Volpe, *Rev. Mod. Phys.* **88**, 045006 (2016).
 [7] W. F. Paxton, K. C. Kistler, C. C. Olmeda, A. Sen, S. K. St. Angelo, Y. Cao, T. E. Mallouk, P. E. Lammert, and V. H. Crespi, *J. Am. Chem. Soc.* **126**, 13424 (2004).
 [8] J. R. Howse, R. A. L. Jones, A. J. Ryan, T. Gough, R. Vafabakhsh, and R. Golestanian, *Phys. Rev. Lett.* **99**, 048102 (2007).
 [9] H.-R. Jiang, N. Yoshinaga, and M. Sano, *Phys. Rev. Lett.* **105**, 268302 (2010).
 [10] I. Theurkauff, C. Cottin-Bizonne, J. Palacci, C. Ybert, and L. Bocquet, *Phys. Rev. Lett.* **108**, 268303 (2012).
 [11] J. Palacci, S. Sacanna, A. P. Steinberg, D. J. Pine, and P. M. Chaikin, *Science* **339**, 936 (2013).
 [12] C. Lozano, B. ten Hagen, H. Löwen, and C. Bechinger, *Nat. Commun.* **7**, 12828 (2016).
 [13] V. Narayan, S. Ramaswamy, and N. Menon, *Science* **317**, 105 (2007).
 [14] S. Ramaswamy, *Annu. Rev. Condens. Matter Phys.* **1**, 323 (2010).
 [15] C. A. Weber, T. Hanke, J. Deseigne, S. Léonard, O. Dauchot, E. Frey, and H. Chaté, *Phys. Rev. Lett.* **110**, 208001 (2013).
 [16] O. Dauchot and V. Démery, *Phys. Rev. Lett.* **122**, 068002 (2019).
 [17] T. Vicsek and A. Zafeiris, *Phys. Rep.* **517**, 71 (2012).
 [18] A. Bricard, J.-B. Caussin, N. Desreumaux, O. Dauchot, and D. Bartolo, *Nature (London)* **503**, 95 (2013).
 [19] J. Elgeti, R. G. Winkler, and G. Gompper, *Rep. Prog. Phys.* **78**, 056601 (2015).
 [20] J. Yan, M. Han, J. Zhang, C. Xu, E. Luijten, and S. Granick, *Nat. Mater.* **15**, 1095 (2016).
 [21] A. Deblais, T. Barois, T. Guerin, P. H. Delville, R. Vaudaine, J. S. Lintuvuori, J. F. Boudet, J. C. Baret, and H. Kellay, *Phys. Rev. Lett.* **120**, 188002 (2018).
 [22] H. Massana-Cid, F. Meng, D. Matsunaga, R. Golestanian, and P. Tierno, *Nat. Commun.* **10**, 2444 (2019).
 [23] H. H. Wensink, J. Dunkel, S. Heidenreich, K. Drescher, R. E. Goldstein, H. Löwen, and J. M. Yeomans, *Proc. Natl. Acad. Sci. U.S.A.* **109**, 14308 (2012).
 [24] G. Kokot, S. Das, R. G. Winkler, G. Gompper, I. S. Aranson, and A. Snezhko, *Proc. Natl. Acad. Sci. U.S.A.* **114**, 12870 (2017).
 [25] I. Buttinoni, J. Bialké, F. Kümmel, H. Löwen, C. Bechinger, and T. Speck, *Phys. Rev. Lett.* **110**, 238301 (2013).
 [26] M. E. Cates and J. Tailleur, *Annu. Rev. Condens. Matter Phys.* **6**, 219 (2015).
 [27] E. Sese-Sansa, I. Pagonabarraga, and D. Levis, *Europhys. Lett.* **124**, 30004 (2018).
 [28] A. P. Solon, Y. Fily, A. Baskaran, M. E. Cates, Y. Kafri, M. Kardar, and J. Tailleur, *Nat. Phys.* **11**, 673 (2015).
 [29] F. Smallenburg and H. Löwen, *Phys. Rev. E* **92**, 032304 (2015).

- [30] X.-L. Wu and A. Libchaber, *Phys. Rev. Lett.* **84**, 3017 (2000).
- [31] D. Loi, S. Mossa, and L. F. Cugliandolo, *Phys. Rev. E* **77**, 051111 (2008).
- [32] S. Krishnamurthy, S. Ghosh, D. Chatterji, R. Ganapathy, and A. K. Sood, *Nat. Phys.* **12**, 1134 (2016).
- [33] L. Angelani, R. Di Leonardo, and G. Ruocco, *Phys. Rev. Lett.* **102**, 048104 (2009).
- [34] R. Di Leonardo, L. Angelani, D. DellArciprete, G. Ruocco, V. Iebba, S. Schippa, M. P. Conte, F. Mecarini, F. De Angelis, and E. Di Fabrizio, *Proc. Natl. Acad. Sci. U.S.A.* **107**, 9541 (2010).
- [35] A. Sokolov, M. M. Apodaca, B. A. Grzybowski, and I. S. Aranson, *Proc. Natl. Acad. Sci. U.S.A.* **107**, 969 (2010).
- [36] S. A. Mallory, C. Valeriani, and A. Cacciuto, *Phys. Rev. E* **90**, 032309 (2014).
- [37] A. Kaiser and H. Löwen, *J. Chem. Phys.* **141**, 044903 (2014).
- [38] J. Harder, C. Valeriani, and A. Cacciuto, *Phys. Rev. E* **90**, 062312 (2014).
- [39] M. Paoluzzi, R. Di Leonardo, M. C. Marchetti, and L. Angelani, *Sci. Rep.* **6**, 34146 (2016).
- [40] N. Nikola, A. P. Solon, Y. Kafri, M. Kardar, J. Tailleur, and R. Voituriez, *Phys. Rev. Lett.* **117**, 098001 (2016).
- [41] G. Junot, G. Briand, R. Ledesma-Alonso, and O. Dauchot, *Phys. Rev. Lett.* **119**, 028002 (2017).
- [42] C. Wang, Y.-k. Guo, W.-d. Tian, and K. Chen, *J. Chem. Phys.* **150**, 044907 (2019).
- [43] W. Gao, A. Pei, X. Feng, C. Hennessy, and J. Wang, *J. Am. Chem. Soc.* **135**, 998 (2013).
- [44] P. Dolai, A. Simha, and S. Mishra, *Soft Matter* **14**, 6137 (2018).
- [45] L. Angelani, *J. Phys. Condens. Matter* **31**, 075101 (2019).
- [46] S. C. Takatori and J. F. Brady, *Soft Matter* **11**, 7920 (2015).
- [47] J. Stenhammar, R. Wittkowski, D. Marenduzzo, and M. E. Cates, *Phys. Rev. Lett.* **114**, 018301 (2015).
- [48] S. Asakura and F. Oosawa, *J. Chem. Phys.* **22**, 1255 (1954).
- [49] M. D. Gratale, T. Still, C. Matyas, Z. S. Davidson, S. Lobel, P. J. Collings, and A. G. Yodh, *Phys. Rev. E* **93**, 050601(R) (2016).
- [50] S. Sacanna, W. T. M. Irvine, P. M. Chaikin, and D. J. Pine, *Nature (London)* **464**, 575 (2010).
- [51] G. Meng, N. Arkus, M. P. Brenner, and V. N. Manoharan, *Science* **327**, 560 (2010).
- [52] G. H. Koenderink, G. A. Vliegenthart, S. G. J. M. Kluijtmans, A. van Blaaderen, A. P. Philipse, and H. N. W. Lekkerkerker, *Langmuir* **15**, 4693 (1999).
- [53] A. Stradner, H. Sedgwick, F. Cardinaux, W. C. K. Poon, S. U. Egelhaaf, and P. Schurtenberger, *Nature (London)* **432**, 492 (2004).
- [54] L. Angelani, C. Maggi, M. L. Bernardini, A. Rizzo, and R. Di Leonardo, *Phys. Rev. Lett.* **107**, 138302 (2011).
- [55] J. Harder, S. A. Mallory, C. Tung, C. Valeriani, and A. Cacciuto, *J. Chem. Phys.* **141**, 194901 (2014).
- [56] R. C. Krafnick and A. E. García, *Phys. Rev. E* **91**, 022308 (2015).
- [57] D. Ray, C. Reichhardt, and C. J. Olson Reichhardt, *Phys. Rev. E* **90**, 013019 (2014).
- [58] R. Ni, M. A. Cohen Stuart, and P. G. Bolhuis, *Phys. Rev. Lett.* **114**, 018302 (2015).
- [59] L. R. Leite, D. Lucena, F. Q. Potiguar, and W. P. Ferreira, *Phys. Rev. E* **94**, 062602 (2016).
- [60] M. Z. Yamchi and A. Naji, *J. Chem. Phys.* **147**, 194901 (2017).
- [61] A. Duzgun and J. V. Selinger, *Phys. Rev. E* **97**, 032606 (2018).
- [62] Y. Hua, K. Li, X. Zhou, L. He, and L. Zhang, *Soft Matter* **14**, 5205 (2018).
- [63] Y. Baek, A. P. Solon, X. Xu, N. Nikola, and Y. Kafri, *Phys. Rev. Lett.* **120**, 058002 (2018).
- [64] See the Supplemental Material at <http://link.aps.org/supplemental/10.1103/PhysRevLett.124.158001> for additional experimental and simulation details, which includes Refs. [65–70].
- [65] C. Reichhardt and C. J. Olson Reichhardt, *Phys. Rev. E* **88**, 062310 (2013).
- [66] A. J. Paine, W. Luymes, and J. McNulty, *Macromolecules* **23**, 3104 (1990).
- [67] J. C. Crocker and D. G. Grier, *J. Colloid Interface Sci.* **179**, 298 (1996).
- [68] K. C. Neuman and S. M. Block, *Rev. Sci. Instrum.* **75**, 2787 (2004).
- [69] D. El Masri, P. van Oostrum, F. Smallenburg, T. Vissers, A. Imhof, M. Dijkstra, and A. van Blaaderen, *Soft Matter* **7**, 3462 (2011).
- [70] T. A. Nieminen, V. L. Y. Loke, A. B. Stilgoe, G. Knöner, A. M. Brańczyk, N. R. Heckenberg, and H. Rubinsztein-Dunlop, *J. Opt. A* **9**, S196 (2007).
- [71] M. Yang and M. Ripoll, *J. Phys. Condens. Matter* **24**, 195101 (2012).
- [72] Y. Fily, A. Baskaran, and M. F. Hagan, *Soft Matter* **10**, 5609 (2014).